

Synthetic data shuffling accelerates the convergence of federated learning under data heterogeneity

Bo Li* Yasin Esfandiari Mikkel N. Schmidt Tommy S. Alstrøm
DTU[†] CISPA[‡] DTU[†]
bli@dtu.dk yasin.esfandiari@cispa.de {mncs, tsal}@dtu.dk

Sebastian U. Stich
CISPA[‡]
stich@cispa.de

Abstract

In federated learning, data heterogeneity is a critical challenge. A straightforward solution is to shuffle the clients' data to homogenize the distribution. However, this may violate data access rights, and how and when shuffling can accelerate the convergence of a federated optimization algorithm is not theoretically well understood. In this paper, we establish a precise and quantifiable correspondence between data heterogeneity and parameters in the convergence rate when a fraction of data is shuffled across clients. We prove that shuffling can quadratically reduce the gradient dissimilarity with respect to the shuffling percentage, accelerating convergence. Inspired by the theory, we propose a practical approach that addresses the data access rights issue by shuffling locally generated synthetic data. The experimental results show that shuffling synthetic data improves the performance of multiple existing federated learning algorithms by a large margin.

1 Introduction

Federated learning (FL) is emerging as a fundamental distributed learning paradigm that allows a central server model to be learned collaboratively from distributed clients without ever requesting the client data, thereby dealing with the issue of data access rights [20, 12, 41, 35]. One of the most popular algorithms in FL is FedAvg [20]. A server distributes a model to the participating clients, who then update it with their local data for multiple steps before communicating it to the server, where the received client models are aggregated, finishing one round of communication. Two main challenges in FedAvg optimization are 1) large data heterogeneity across clients and 2) limited available data on each client [20].

Data heterogeneity refers to differences in data distributions among participating clients [12]. Existing works typically characterize its impact on the convergence of FedAvg using bounds on the gradient dissimilarity, which suggests a slow convergence when the data heterogeneity is high [14, 19]. Many efforts have been made to improve FedAvg's performance in this setting using advanced techniques such as control variates [14, 2, 23] and regularizers [43]. Although these algorithms have demonstrated great success in many applications, they are insufficient under high data heterogeneity [48]. On the other hand, many researchers [51, 44] observed that simply augmenting the dataset on each client with a small portion of shuffled data collected from all clients can significantly accelerate the convergence of FedAvg. However, it has yet to be well understood when and, in particular, by how much shuffling can accelerate the convergence.

Another challenge arises when the amount of available data on each client is limited, especially when the number of classes or tasks is large. High-capacity deep neural networks (DNN) usually require

*Work done while at CISPA

[†]Technical University of Denmark

[‡]CISPA Helmholtz Center for Information Security

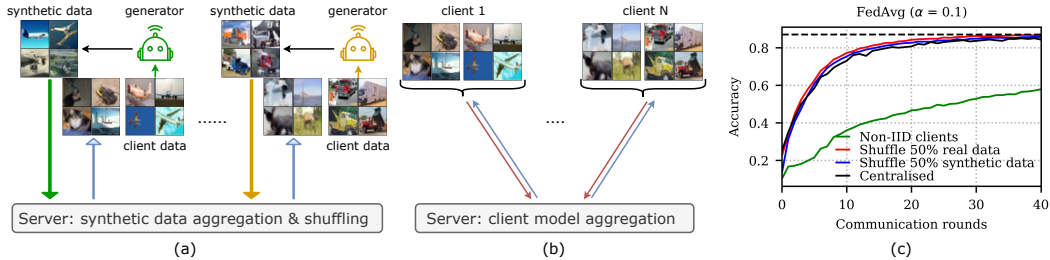


Figure 1: Our proposed framework. (a) Each client learns a generator with a subset of its local data and generates synthetic data, which are communicated to the server. The server then shuffles and redistributes the collection of the synthetic data to each client. (b) With the updated client dataset, any FL algorithms can be used to learn a server model. (c) When the clients are very heterogeneous, compared to collecting, shuffling, and redistributing the real data, shuffling synthetic data achieves a similar accuracy while alleviating information leakage.

large-scale labelled datasets to avoid overfitting [10, 37]. However, labelled data acquisition can be expensive and time-consuming [37]. Therefore, learning with conditionally generated synthetic samples has been an active area of research [34, 8, 37, 49, 52, 24]. Adapting the framework of using synthetic data from centralized learning to FL is not trivial due to the unique properties of FL, such as distributed datasets, high communication costs, and privacy requirements [12].

In this work, we provide a more precise and quantifiable correspondence between data heterogeneity and the parameters in the convergence rate. Specifically, we prove that reducing data heterogeneity by shuffling in a small percentage of data from existing clients gives a quadratic reduction in the gradient dissimilarity and can lead to a super-linear reduction in the number of communication rounds. The number of rounds is reduced by a factor greater than the shuffle percentage. Further, we show that the theory holds in both strongly-convex functions and non-convex DNN-based FL.

While our theory suggests that shuffling even a small percentage of clients’ data can reduce the required communication rounds to reach certain accuracy, collecting real data from clients goes against the goal of protecting privacy in FL. Therefore, we propose a more practical framework Fedssyn where we shuffle a collection of synthetic data from all the clients at the beginning of FL (see Fig. 1). Each client learns a client-specific generator with a subset of its local data and generates synthetic data. The server then receives, shuffles, and redistributes the synthetic data to each client. This process only happens once and has no requirements on the FL algorithm that is being used.

Contributions: We summarize our main results below:

- We rigorously analyze the relation between data heterogeneity and the parameters in the convergence rate in FedAvg. We prove that shuffling a small percentage of data across clients gives a quadratic reduction in the gradient dissimilarity and can lead to a super-linear reduction in the number of communication rounds. We empirically verify the tightness of the theory on strongly convex and DNN-based non-convex functions.
- We present a practical framework Fedssyn, that shuffles locally generated synthetic data and can be coupled with *any* FL algorithms.
- We empirically demonstrate that using Fedssyn on top of several popular FL algorithms reduces the number of communication rounds and improves Top-1 accuracy. Results hold across multiple datasets, different levels of data heterogeneity, number of clients, and participation rates.

1.1 Related work

Federated optimization: FL is a fast-growing field [12, 41]. We here mainly focus on works that address the optimization problems in FL. FedAvg [20] is one of the most commonly used optimization techniques. Despite its success in many applications, its convergence performance under heterogeneous data is still an active area of research [14, 42, 16, 32, 44, 23]. Theoretical results suggest that the *drift* caused by the data heterogeneity has a strong negative impact on FedAvg convergence. However, in practice, the impact of data heterogeneity is often less detrimental than the theory has predicted, especially in DNN-based FL [14, 32, 4].

Several lines of work have been proposed to reduce the impact of data heterogeneity, including regularizers [32], control variates for correcting gradients [14, 2, 23, 30], and decoupled representation and classification [7, 26, 48]. However, such methods are insufficient to conquer high client heterogeneity and can hardly achieve comparable accuracies as in the IID scenarios [48]. Other works proposed to use sophisticated aggregation strategies on the server via ensemble distillation [25], momentum [13], normalization [43], or adaptivity [31].

Synthetic data-based FL: Many works attempt to improve the performance of FL algorithms using synthetic datasets [46, 52, 49, 24, 8, 40]. These works can be grouped into 1) client-generator [46, 24, 40], where synthetic data is generated locally and then communicated to the server for the server model updating, and 2) server-generator [52, 49], where a centralized generator is used to assist in updating the server and/or client model. Compared to the existing synthetic data-based FL methods, our proposed framework is simple to use, requires less additional communication cost, and has removed many other complicated components, as shown in Table A.1.

Generative models: Generative models can be trained to mimic the underlying distribution of complex data modalities such as text and images [9]. Among the existing approaches, Generative Adversary Network (GANs) have achieved great success in generating high-quality, smooth, and sharp images [38, 50, 15]; however, GANs are challenging to train [33], which can especially be an issue in FL as each client has limited data [20]. Recently, diffusion models [11] have attracted much attention due to the high diversity and quality of the generated samples [34], training efficiency [11], and consistency in hyperparameter choices across datasets [34]. Therefore, we study to use DDPM as our local generator in this paper.

Differentially private learning in neural networks: Differential privacy (DP) bounds the influence of any single input on the output of machine learning algorithms to avoid information leakage about the input data [29, 36, 1]. Differentially private stochastic gradient descent (DP-SGD) achieves DP guarantee by clipping gradients and adding random noise [29], which has been applied for training FL algorithms [29] and generative models [45, 5, 47]. However, this paper aims to analyze the relationship between data heterogeneity and convergence rate from the optimization perspective. Using both DP-generator and DP-FL algorithms complicates the problem as it introduces many other variates, such as the clipped gradients and DP-noise. Therefore, we leave this as our future work.

2 Influence of the data heterogeneity on the convergence rate

We formalize the problem as minimizing a sum of stochastic functions with only access to stochastic samples:

$$f^* := \min_{\mathbf{x} \in \mathbb{R}^d} \left[f(\mathbf{x}) := \frac{1}{N} \sum_{i=1}^N f_i(\mathbf{x}) \right], \quad f_i(\mathbf{x}) := \mathbb{E}_{\xi \sim \mathcal{D}_i} F_i(\mathbf{x}; \xi), \quad (1)$$

where \mathcal{D}_i represents the data distribution on client i , f_i represents the loss function on client i with N workers. We assume bounded noise and gradient dissimilarity following [19, 39]:

Assumption 1 (gradient dissimilarity). *We assume that there exists ζ^2 such that $\forall \mathbf{x} \in \mathbb{R}^d$:*

$$\mathbb{E} \|\nabla f_i(\mathbf{x}) - \nabla f(\mathbf{x})\|^2 \leq \zeta^2. \quad (2)$$

That is, ζ^2 represents the diversity of the objective functions f_i among clients.

Assumption 2 (stochastic noise). *We assume that there exists σ^2 such that $\forall \mathbf{x} \in \mathbb{R}^d$:*

$$\mathbb{E}_{\xi \sim \mathcal{D}_i} \|\nabla F_i(\mathbf{x}; \xi) - \nabla f_i(\mathbf{x})\|^2 \leq \sigma^2. \quad (3)$$

That is, σ^2 measures the stochastic noise in (minibatch) gradient estimates.

2.1 Motivation

In real-world FL applications, each client often collects data individually, so data heterogeneity across clients is unavoidable [6, 20]. Experimental studies often simulate data heterogeneity by limiting the number of classes (tasks) on each client by splitting data into shards (Shards-sampling) [20, 48] or using Dirichlet sampling based on a concentration parameter α (Dirichlet-sampling) [2, 25, 23]. It has been observed in both sampling schemes that under high data heterogeneity, replacing a small percentage of the client’s data, e.g. 10%, with data shuffled across clients, can enormously reduce the

reached optimal error [44, 51]. However, this empirically vast improvement due to shuffling has yet to be well explained by theory. Therefore, we aim to fill this gap in the following sections.

To formally describe the data heterogeneous scenario, we assume each client has access to data with distribution \mathcal{D}_i that is non-iid across clients and we denote by $\tilde{\mathcal{D}} := \bigcup_i \mathcal{D}_i$ the uniform distribution over the joint data. We can now model our shuffling scenario where the server mixes and redistributes a small p fraction of the data by introducing new client distributions $\hat{\mathcal{D}}_i := (1-p)\mathcal{D}_i + p\tilde{\mathcal{D}}$ for a shuffling parameter $p \in [0, 1]$. If $p = 0$, the local data remains unchanged, and if $p = 1$, the data is uniform across clients. This formulation is consistent with the `Shards-sampling` and `Dirichlet-sampling` as we can choose p to match the corresponding degree of data heterogeneity.

2.2 Theoretical analysis

We extend the analysis from [19, 44, 17], which qualitatively characterizes the impact of data heterogeneity on FedAvg, to incorporate a more quantifiable relation between data heterogeneity and parameters in the convergence rate. Namely, shuffling p fraction of data to each client reduces gradient dissimilarity quadratically and can significantly accelerate the convergence when the stochastic noise is small. We describe this in detail next.

Lemma 1. *If Assumption 1 and 2 hold, $\forall \mathbf{x} \in \mathbb{R}^d$ given p as the fraction of shuffled data on each client, the effective stochastic noise $\hat{\sigma}_p^2$, the gradient dissimilarity $\hat{\zeta}_p^2$ and the smoothness constant L_p (the maximal smoothness constant of each client function f_i after shuffling), satisfy in expectation:*

$$\mathbb{E}\hat{\sigma}_p^2 \leq (1-p)\sigma^2 + p\tilde{\sigma}^2 + p(1-p)\zeta^2, \quad \mathbb{E}\hat{\zeta}_p^2 \leq (1-p)^2\zeta^2, \quad \mathbb{E}L_p \leq (1-p)L_{\max} + pL_{\text{avg}}, \quad (4)$$

where $\tilde{\sigma}^2$ denotes the stochastic noise on the shuffled data ($p = 1$), σ^2 and ζ^2 denote the stochastic noise, the gradient dissimilarity and the smoothness using the initial local data \mathcal{D}_i (e.g. $p = 0$) and L_{avg} and L_{\max} denote the average and maximal smoothness across all individual loss functions $F_i(\mathbf{x}; \xi)$.

Lemma 1 shows the effective stochastic noise and gradient dissimilarity when each client i contains a fraction p of shuffled data (see Appendix D for the proof). We observe that the gradient dissimilarity decays quadratically with respect to p . When $p = 1$, the gradient dissimilarity is 0 as expected, since data is iid across workers, $f_i = f_j, \forall i \neq j$. Additionally, we can see that the effective stochastic noise is affected by both stochastic noise and gradient dissimilarity. We now demonstrate the impact of these parameters on the convergence by utilizing the convergence bounds established in [19, 44, 17] and combining them with our Lemma 1:

Corollary I (Convergence rate after shuffling). *We consider: p as the fraction of shuffled data on each client; $\tilde{\sigma}^2$ as the stochastic noise on the shuffled data; τ as local steps; and $\{f_i\}$ are L_1 -smooth, under Assumption 1 and 2, for any target accuracy $\epsilon > 0$, there exists a (constant) stepsize such that the accuracy can be reached after at most T iterations (in expectation):*

Strongly-convex:

$$T = \mathcal{O} \left(\frac{(1-p)\sigma^2 + p\tilde{\sigma}^2 + p(1-p)\zeta^2}{\mu N \epsilon} + \frac{\sqrt{L_p} (\tau(1-p)\zeta + \sqrt{\tau} \sqrt{(1-p)\sigma^2 + p\tilde{\sigma}^2 + p(1-p)\zeta^2})}{\mu \sqrt{\epsilon}} + \frac{L_p \tau}{\mu} \log \frac{1}{\epsilon} \right)$$

Non-convex:

$$T = \mathcal{O} \left(\frac{L_p ((1-p)\sigma^2 + p\tilde{\sigma}^2 + p(1-p)\zeta^2)}{N \epsilon^2} + \frac{L_p (\tau(1-p)\zeta + \sqrt{\tau} \sqrt{(1-p)\sigma^2 + p\tilde{\sigma}^2 + p(1-p)\zeta^2})}{\epsilon^{3/2}} + \frac{L_p \tau}{\epsilon} \right)$$

Without shuffling, e.g. $p = 0$, [19] demonstrate the convergence rate of FedAvg as:

$$\text{Strongly-convex: } \mathcal{O} \left(\frac{\sigma^2}{N \mu \epsilon} + \frac{\sqrt{L_1} (\tau \zeta + \sqrt{\tau} \sigma)}{\mu \sqrt{\epsilon}} + \frac{L_1 \tau}{\mu} \log \frac{1}{\epsilon} \right), \quad \text{Non-convex: } \mathcal{O} \left(\frac{L_1 \sigma^2}{N \epsilon^2} + \frac{L_1 (\tau \zeta + \sqrt{\tau} \sigma)}{\epsilon^{3/2}} + \frac{L_1 \tau}{\epsilon} \right).$$

From Corollary I, we see that if $\sigma^2 > 0$, the convergence rate is asymptotically dominated by the first term $\mathcal{O} \left(\frac{(1-p)\sigma^2 + p\tilde{\sigma}^2 + p(1-p)\zeta^2}{n \mu \epsilon} \right)$, which shows a mixed effect between the stochastic noise and the gradient dissimilarity. When the stochastic noise is larger than the gradient dissimilarity and σ^2 and $\tilde{\sigma}^2$ are similar, sampling shuffled data into each client has a negligible effect on the first term.

When $\sigma^2 = 0$, or in general in the early phases of the training (when the target accuracy ϵ is not too small), the convergence is super-linear due to the joint decrease of L_p and ζ_p^2 . Specifically, we observe that as we increase the ratio of the shuffled data p , the number of iterations T to achieve accuracy ϵ is super-linearly reduced as T is proportional to $(1-p)\zeta\sqrt{L_p}$ in expectation for strongly convex functions.

2.3 Illustrative experiments on convex functions

We here focus on verifying that the empirical performance of a FL algorithm matches the provided theoretical results when we shuffle a p fraction of the local data. Following⁴ [19], we consider a distributed least squares objective $f(\mathbf{x}) := \frac{1}{n} \sum_{i=1}^n [f_i(\mathbf{x}) := \frac{1}{2n_i} \sum_{j=1}^{n_i} \|\mathbf{A}_{ij}\mathbf{x} - \mathbf{b}_{ij}\|^2]$ with $\mathbf{A}_{ij} = i\mathbf{I}_d$, $\boldsymbol{\mu}_i \sim \mathcal{N}(0, \zeta^2(id)^{-2}\mathbf{I}_d)$, and $\mathbf{b}_{ij} \sim \mathcal{N}(\boldsymbol{\mu}_i, \sigma^2(id)^{-2}\mathbf{I}_d)$, where ζ^2 controls the function similarity and σ^2 controls the stochastic noise (matching parameters in Corollary I). On each worker, we generate $n_i = 100$ pairs of $\{\mathbf{A}_{ij}, \mathbf{b}_{ij}\}$ with $d = 25$. We randomly sample $p \cdot n_i$ pairs of $\{\mathbf{A}_{ij}, \mathbf{b}_{ij}\}$ from all the clients. We then aggregate, shuffle, and redistribute them equally to each client such that the number of functions per client is still n_i . We depict the influence of shuffling on different parameters in Fig. 2. To concisely match out theory, we need to consider that also the curvature of the function changes and measure L_p , $L_{\max} := \max_i \|\frac{1}{n_i} \sum_{j=1}^{n_i} \mathbf{A}_{ij}^T \mathbf{A}_{ij}\|$ and $L_{\text{avg}} := \frac{1}{n} \sum_{i=1}^n \|\frac{1}{n_i} \sum_{j=1}^{n_i} \mathbf{A}_{ij}^T \mathbf{A}_{ij}\|$. An additional non-convex experiment using MNIST [22] that shows the accumulative effect between local steps and shuffling is shown in the appendix (Fig. B.2).

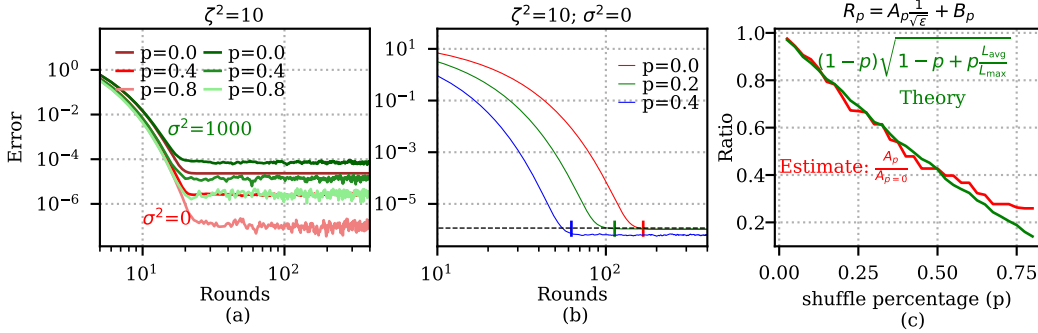


Figure 2: Convergence of $\frac{1}{n} \sum_{i=1}^n \|\mathbf{x}_i^t - \mathbf{x}^*\|^2$. (a) With a fixed ζ^2 and step size, shuffling reduces the optimal error more when the stochastic noise is low (b) When gradient dissimilarity ζ^2 dominates the convergence, we obtain a super-linear speedup in the number of rounds to reach ϵ by shuffling more data. The vertical bar shows the theoretical number of rounds to reach ϵ (c) The estimated ratio matches the theoretical ratio when the shuffle percentage is small (e.g. $p \leq 0.6$). The term $\sqrt{1-p+p\frac{L_{\text{avg}}}{L_{\max}}}$ comes from the Lipschitz constant ratio $\sqrt{\frac{L_p}{L_{p=0}}}$.

Fig. 2 (a) shows the influence of shuffling when we vary the stochastic noise given a fixed ζ^2 and stepsize. We observe that in the high-noise regime, shuffling gives a smaller reduction on the optimal error than when $\sigma^2 = 0$ as $\mathcal{O}\left(\frac{(1-p)\sigma^2+p\bar{\sigma}^2}{\epsilon}\right)$ tends to dominate no matter how much data we shuffle. Fig. 2 (b) shows the influence of shuffling when $\sigma^2 = 0$ and $\mathcal{O}\left(\frac{\sqrt{L_p}\tau(1-p)\zeta}{\sqrt{\epsilon}}\right)$ dominates the convergence. We tune the step size for each experiment to reach the target accuracy ($\epsilon = 1.1 \cdot 10^{-6}$) with the fewest rounds. The theoretical number of rounds required to reach ϵ , indicated by the vertical bars, were determined by calculating $R_p = \frac{A_p}{\sqrt{\epsilon}} + B_p$, where A_p is the coefficient that depends on ζ^2 and L_p . To estimate A_p , we measure the number of rounds to reach different accuracies and fit a linear line between R_p and $\frac{1}{\sqrt{\epsilon}}$. The fitted lines are shown in the Appendix. Fig. 2 (b) shows that the empirical speedup matches the theoretical speedup as the observed and theoretical number of rounds to reach the target accuracy are very close. For better visualization, we compare the theoretical and estimated ratio in Fig. 2 (c) given $\sigma^2 = 0$. Fig. 2(c) shows the ratio between the coefficient $\frac{A_p}{A_{p=0}}$ which boils down to $\mathcal{O}\left(\frac{\sqrt{L_p}\zeta_p}{\sqrt{L_{p=0}\zeta_{p=0}}}\right)$. The nearly matching lines in Fig. 2 (c), especially when p is

⁴In contrast to [19] that consider the online setting, we generate here a finite set of samples on each client.

small, verify our theoretical statement about the impact of data heterogeneity on the convergence parameters. When p is large, σ^2 and the constant term tend to dominate the convergence. A linear line between R_p and $\frac{1}{\sqrt{\epsilon}}$ is incomplete to explain the convergence rate.

3 Synthetic data shuffling

We have theoretically and empirically verified the benefit of adding shuffled data to each client. However, collecting data from all the clients goes against the goal of protecting user privacy in FL. To still enjoy the benefit of shuffling and alleviate information leakage, we propose a practical framework that shuffles the aggregated synthetic data from all the clients (see Fig. 1).

We denote the client dataset, client generated synthetic dataset, and shuffled synthetic dataset by \mathcal{D}_i , $\tilde{\mathcal{D}}_i$, and $\tilde{\mathcal{D}}$ (in accordance with the notation for the data distributions in Sec. 2). On each client i , we uniformly subsample $\rho \cdot n_i$ data points from the local dataset \mathcal{D}_i , given $\rho \in (0, 1]$ and $n_i = |\mathcal{D}_i|$, which we use to locally train a class-conditional generator. Using a subset rather than the entire dataset can alleviate the exposure of the class distribution from each client. Given the trained local generator, we generate $\tilde{\mathcal{D}}_i$ with $|\tilde{\mathcal{D}}_i| = \tilde{n}$ synthetic data, matching the class frequency in the subset. We assume that all the clients are willing to send their synthetic dataset to the server. The server then shuffles the aggregated synthetic datasets $\bigcup_{i \in [N]} \tilde{\mathcal{D}}_i$ and distributes the data uniformly among the clients. In practice, when the number of synthetic data is large, their statistical dependency is negligible, and the synthetic data can be considered nearly iid. Reflecting this, we denote the *partitioned* shuffled synthetic dataset as $\tilde{\mathcal{D}}_{si}$ on each client, and the proportion of the synthetic dataset is calculated as $p := \frac{\tilde{n}}{n_i + \tilde{n}}$ (see Algorithm I).

We then run FL algorithms with the updated dataset on each client $\mathcal{D}_i \cup \tilde{\mathcal{D}}_{si}$. Our framework has no requirements for the FL algorithm, so we here briefly describe one of the most common FL algorithms: FedAvg [20], as shown in Algorithm II. FedAvg mainly has two steps: local model updating and server aggregating. We initialize the server with a model \mathbf{x} . In each communication round, each participating client $S \subseteq [N]$ receives a copy of the server parameter \mathbf{x} and performs K steps local updates (e.g. K steps SGD). The updated model \mathbf{y}_i is then sent to the server. FedAvg calculates the server model by averaging over the received client models, finishing one round of communication. We repeat this for R rounds or until the target accuracy is achieved.

Algorithm I Fedssyn

```

1: procedure SYNTHETIC DATA GENERATION
2:   for client  $i = 1, \dots, N$  in parallel do
3:     sample  $\rho \cdot n_i$  data points from  $\mathcal{D}_i$ 
4:     train a generator  $\mathcal{G}_i$ 
5:     generate  $\tilde{\mathcal{D}}_i$  with  $\tilde{n}$  samples
6:     Communicate  $\tilde{\mathcal{D}}_i$  to the server
7:   end for
8:   Server shuffles the aggregated synthetic data  $\{\tilde{\mathcal{D}}_1, \dots, \tilde{\mathcal{D}}_N\}$  and split it to  $N$  parts ( $\{\tilde{\mathcal{D}}_{si}\}$ )
9:   Server distributes  $\tilde{\mathcal{D}}_{si}$  ( $|\tilde{\mathcal{D}}_{si}| = \tilde{n}$ ) to each client
10:  Run FL algorithm with the updated client dataset on each client  $\hat{\mathcal{D}}_i := \mathcal{D}_i \cup \tilde{\mathcal{D}}_{si}$ 
11: end procedure

```

Algorithm II Federated Averaging (FedAvg)

```

1: procedure FEDAVG
2:   for  $r = 1, \dots, R$  do
3:     Sample clients  $S \subseteq \{1, \dots, N\}$ 
4:     Send server model  $\mathbf{x}$  to all clients  $i \in S$ 
5:     for client  $i \in S$  in parallel do
6:       initialise local model  $\mathbf{y}_i \leftarrow \mathbf{x}$ 
7:       for  $k = 1, \dots, K$  do
8:          $\mathbf{y}_i \leftarrow \mathbf{y}_i - \eta \nabla F_i(\mathbf{y}_i)$ 
9:       end for
10:    end for
11:     $\mathbf{x} \leftarrow \mathbf{x} + \frac{1}{|S|} \sum_{i \in S} (\mathbf{y}_i - \mathbf{x})$ 
12:  end for
13: end procedure

```

4 Experimental setup

We demonstrate the effectiveness of our proposed method on CIFAR10 and CIFAR100 [21] image classification tasks. We leave the test set on the server to evaluate the accuracy of the server model. We partition the training dataset using Dirichlet distribution with a concentration parameter α to simulate the heterogeneous scenarios following [25]. The smaller the α , the higher data heterogeneity among the clients. We choose $\alpha \in \{0.01, 0.1\}$ in our study as they are commonly used [48, 25]. Each client has a local dataset, kept fixed and local throughout the communication rounds.

We use DDPM [11] with the same architecture as [11] as our class-conditional generator on each client due to its training efficiency and consistency in hyperparameter choices across datasets [34].

We assume that all the clients participate in training DDPM by using 75% of their local data as the training data. Each client trains DDPM with a learning rate of 0.0001, 1000 diffusion time steps, 256 batch size, and 500 epochs. These hyperparameters are the same for all experiments. Once the training finishes, each client simulates $\tilde{n} = \frac{50000}{N}$ (there are 50K training images in CIFAR10 and CIFAR100) synthetic images with the label, which are then sent to the server. The server aggregates and shuffles the received synthetic dataset and then distributes it to each client equally. This finishes the synthetic data generation and distribution process.

We then perform federated optimization. We experiment with some of the popular FL algorithms including FedAvg [20], FedProx [32], SCAFFOLD [14], FedDyn [2], and FedPVR [23]. We use VGG-11 for all the experiments. We train the FL algorithm with and without using the synthetic dataset to demonstrate the speedup obtained from using synthetic dataset quantitatively.

We experiment with full and partial clients participation. We use $N \in \{10, 40, 100\}$ as the number of clients and $C \in \{0.1, 0.2, 0.4, 1.0\}$ as the participation rate. For partial participation, we randomly sample $N \cdot C$ clients per communication round. For all the experiments, we use a batch size of 256, 10 local epochs, and the number of gradient steps $\frac{10n_i}{256}$. We tune the client learning rate from $\{0.01, 0.05, 0.1\}$ with the local validation dataset (10% of the training data). The learning rate is the same along the communication rounds. The results are given as an average of three repeated experiments with different random initializations. The code is publically available at <https://github.com/lyn1874/fedssyn>.

5 Experimental results

We demonstrate the performance of Fedssyn on top of five popular FL frameworks here. Our main findings are: 1) Sampling shuffled synthetic data into each client can significantly reduce the number of rounds used to reach a target accuracy and increase the Top-1 accuracy. 2) The performance across different FL algorithms is nearly identical when we use the shuffled synthetic data. 3) The quantified gradient dissimilarity and stochastic noise in DNN match the theoretical statements.

5.1 Communication efficiency and accuracy

We first report the required number of communication rounds to reach the target accuracy in Table 1. The length of the grey and red colour bar represents the required number of rounds to reach accuracy m when the local dataset is \mathcal{D}_i and $\mathcal{D}_i \cup \tilde{\mathcal{D}}_{si}$, respectively. The speedup is the ratio between the number of rounds in these two settings. We observe that adding shuffled synthetic data to each client can reduce the number of communication rounds to reach the target accuracy for all the FL algorithms, datasets, data heterogeneity levels, and different participation rates. Additionally, we see the speedup is small when the number of clients is high on CIFAR100, *e.g.* $N = 100$. One of the main reasons is that the quality of the generator drops as the number of images used to train the local generator is small (375 images), but the number of classes is large (100).

We next report the Top-1 accuracy in Fig. 3. To verify that the accuracy improvement is mainly due to the changes in the convergence parameters rather than the increased number of images on each client, we compare experiments where the local dataset is \mathcal{D}_i , the mixture between local real and local synthetic data $\mathcal{D}_i \cup \tilde{\mathcal{D}}_i$, the mixture between local real and shuffled synthetic data $\mathcal{D}_i \cup \tilde{\mathcal{D}}_{si}$. We also compare them with the centralised experiments using the centralised real and synthetic data.

Fig. 3 shows that using the shuffled synthetic data can significantly improve the Top-1 accuracy in nearly all the cases compared to other baselines, which indicates that the vast performance improvement is mainly due to the changes in the parameters in the convergence rate rather than the increased number of images in each client. Specifically, we observe that the performance differences between different levels of data heterogeneity for the same dataset are nearly negligible (the red bar vertically) when we add the shuffled synthetic data, which indicates that the quality of the generator DDPM is less sensitive to the imbalanced data as it aims at learning the underlying data distribution. We also see that the Top-1 performance is decreasing as we increase the number of clients, especially for the CIFAR100 dataset with 100 clients (the red bar horizontally). We can improve this performance by generating more synthetic images for the CIFAR100 dataset, as 1000 training images (500 real+500 synthetic) per client is insufficient to learn 100 classes.

Table 1: The required number of rounds to reach target accuracy m . The length of the grey and red bar equals to the number of rounds for experiments without the synthetic dataset (\mathcal{D}_i) and with the shuffled synthetic dataset ($\mathcal{D}_i \cup \tilde{\mathcal{D}}_{si}$), respectively. We annotate the length of the red bar, and the speedup (x) is the ratio between the number of rounds in these two settings. “>” means experiments with \mathcal{D}_i as the local data cannot reach accuracy m within 100 communication rounds. Using shuffled synthetic dataset reduces the required number of communication round to reach the target accuracy in all cases.

	Full participation				Partial participation			
	N=10		N=10 (C=40%)		N=40 (C=20%)		N=100 (C=10%)	
	$\alpha = 0.01$	$\alpha = 0.1$	$\alpha = 0.01$	$\alpha = 0.1$	$\alpha = 0.01$	$\alpha = 0.1$	$\alpha = 0.01$	$\alpha = 0.1$
CIFAR10								
	m = 44%	m = 66%	m = 44%	m = 66%	m = 44%	m = 66%	m = 44%	m = 66%
FedAvg	4(22x)	8(8.5x)	4(> 25x)	8(5.6x)	12(8.3x)	21(2.8x)	19(4.9x)	38(> 2.6x)
Scaffold	4(9.3x)	7(6.1x)	5(> 20x)	10(2.6x)	12(6.8x)	20(2.7x)	19(> 5.3x)	31(2.7x)
FedProx	4(23.5x)	8(5.3x)	4(> 25x)	9(8.2x)	9(> 11.1x)	15(4.7x)	31(> 3.2x)	37(> 2.7x)
FedDyn	3(16.3x)	5(14.8x)	4(16.8x)	7(10.7x)	7(> 14.3x)	12(> 5.3x)	17(> 5.9x)	31(> 3.2x)
FedPVR	3(19.3x)	7(4.3x)	4(> 25x)	8(9.5x)	10(8.5x)	21(2.8x)	21(> 4.8x)	35(> 2.9x)
CIFAR100								
	m = 30%	m = 40%	m = 20%	m = 20%	m = 30%	m = 40%	m = 30%	m = 30%
FedAvg	15(5.9x)	19(> 5.2x)	17(> 5.9x)	21(> 4.8x)	37(> 2.7x)	89(> 1.1x)	70(> 1.4x)	59(> 1.7x)
Scaffold	14(2.9x)	19(2.9x)	15(3.6x)	21(4.8x)	24(> 4.2x)	71(> 1.4x)	61(1.6x)	52(> 1.9x)
FedProx	17(5.9x)	23(4.3x)	17(> 5.6x)	23(> 4.3x)	33(> 3.0x)	100 + (-)	75(> 1.3x)	60(> 1.7x)
FedDyn	10(3.6x)	12(5.5x)	13(> 7.7x)	15(6.7x)	25(> 4x)	78(> 1.3x)	61(> 1.6x)	60(> 1.7x)
FedPVR	14(6.1x)	19(2.0x)	15(> 6.6x)	20(5.0x)	23(> 4.3x)	59(> 1.7x)	71(> 1.4x)	58(> 1.7x)

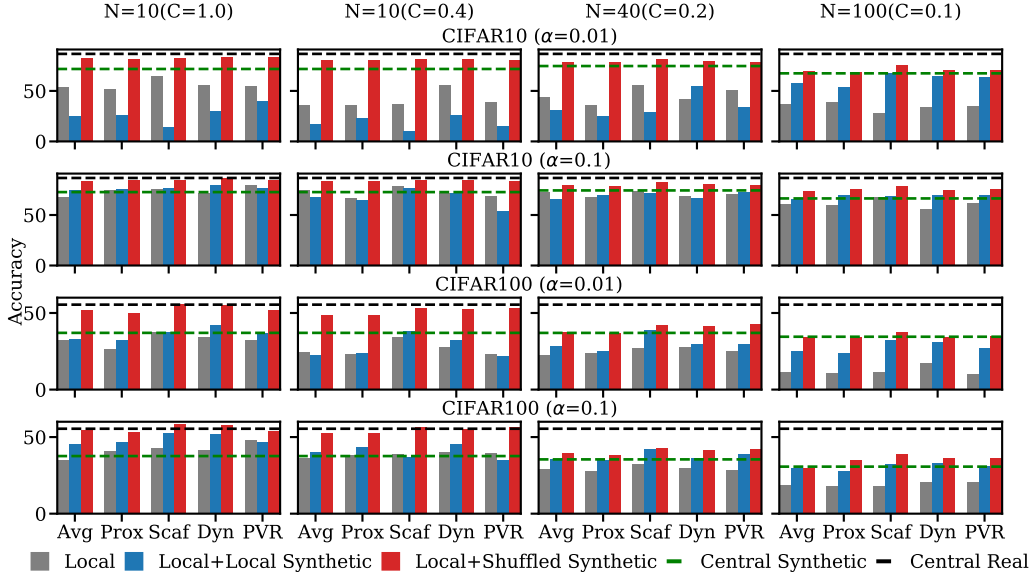


Figure 3: Top-1 accuracy. We compare the experiments where the local dataset is \mathcal{D}_i , $(1-p)\mathcal{D}_i + p\tilde{\mathcal{D}}_i$ (local+local synthetic data), and $(1-p)\mathcal{D}_i + p\tilde{\mathcal{D}}_{si}$ (local+shuffled synthetic data). The black and green dotted lines represent the accuracy using the centralised real and synthetic data, respectively. Using shuffled synthetic data (red bar) boosts the Top-1 accuracy, and in some cases even matches the centralised accuracy.

5.2 Sensitivity analysis

We here depict the sensitivity of FedAvg on the quality of the synthetic data using CIFAR10 in Fig. 4. Fig. 4 (a) shows that the number of images for training DDPM has a substantial impact on FL performance, which is reasonable, as we can acquire higher-quality synthetic images if we use more images to train the generator. Fig. 4 (b) shows that when the number of clients is low, the synthetic images extracted from the early training checkpoints already have high quality. However, when the number of clients is high, the longer we train the generator, the better FL performance we can achieve. Fig. 4 (c) shows that using DDPM is slightly better than GAN-based generators (NDA [38], DGAN and DCrGAN [50], and StyleGAN [15]) in terms of accuracy.

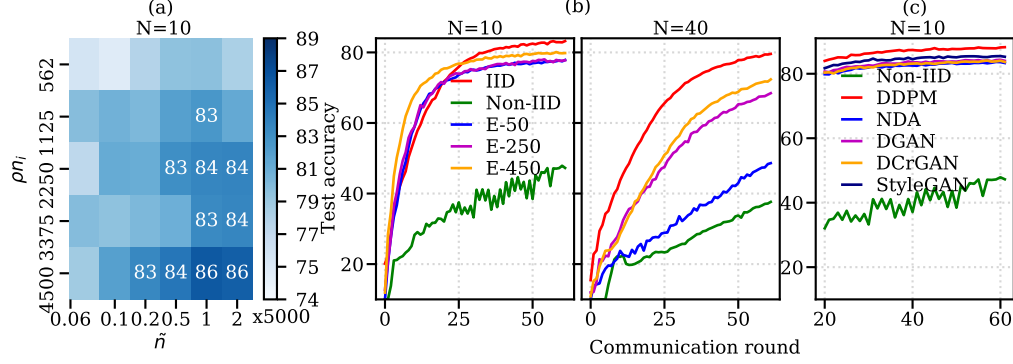


Figure 4: Sensitivity analysis using FedAvg and CIFAR10: (a) the influence of the number of images used for training the generator $\rho \cdot n_i$ and the number of synthetic images per client \tilde{n} ($\alpha = 0.1$). We annotate the combination that performs better than the centralized baseline (b) the influence of the number of training epochs for the generator with 10 and 40 clients ($\alpha=0.01$). (c) the influence of using different generators ($\alpha = 0.01$)

5.3 Parameters in the convergence rate

We here investigate the impact of using shuffled synthetic data on the parameters in the convergence rate for DNN-based FedAvg in Fig. 5. We use CIFAR10, 10 clients with full participation, $\alpha = 0.1$, and $\rho \cdot n_i = 4500$. We observe that when $p = 0.06$, though the stochastic noise $\hat{\sigma}_p^2$ remains similar, $\hat{\zeta}_p^2$ has reduced by half and we improve the Top-1 accuracy by 20%. When $p = 0.5$, we obtain a much smaller $\hat{\sigma}_p^2$ and $\hat{\zeta}_p^2$. Consequently, we achieve an even better Top-1 accuracy than the IID experiment. However, the parameters in Fig. 5 (b) and (c) are evaluated with different server models $x_{p,r}$, so it is less comparable to Lemma 1 where they are measured with the same server model. Therefore, we evaluate the gradient dissimilarity $\hat{\zeta}_p^2$ and stochastic noise $\hat{\sigma}_p^2$ using $\mathcal{D}_i \cup \tilde{\mathcal{D}}_{s_i}$ and the corresponding σ^2 and ζ^2 using \mathcal{D}_i with the same server model x_r in each round in Fig. 5 (d). We use δ to represent how well the distribution of the synthetic data matches the real dataset. See Appendix D for a better explanation. We observe that $(1-p)\sigma^2$ dominates over other terms in the effective stochastic noise, which means the first term in the convergence rate for non-convex function in Corollary I can be simplified as $\mathcal{O}\left(\frac{(1-p)\sigma_p^2 L_p}{n\epsilon^2}\right)$ in this experimental setup. For $\hat{\zeta}_p^2$, the empirical result also matches the theory. These results show that in this experimental setup, adding shuffled synthetic dataset reduces both stochastic noise and function dissimilarity, and lead to a greater accuracy improvement.

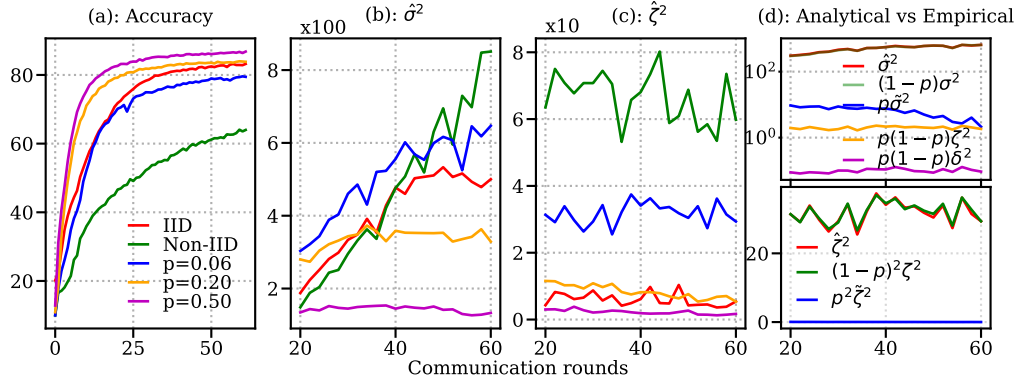


Figure 5: Influence of using shuffled synthetic dataset on the stochastic noise $\hat{\sigma}^2$ and function dissimilarity $\hat{\zeta}^2$ (CIFAR10, 10 clients, $\alpha = 0.1$). The percentage of shuffled data in (d) is 0.06. The empirical observation of $\hat{\sigma}^2$ and $\hat{\zeta}^2$ matches the theoretical statements.

6 Conclusion

In this paper, we have rigorously analyzed the relation between data heterogeneity and the parameters in the convergence rate in FedAvg under standard stochastic noise and gradient dissimilarity assumptions. While previous works usually qualitatively represent data heterogeneity with gradient dissimilarity, we proposed a more quantifiable and precise characterization of how the changes in the data heterogeneity impact the parameters in the convergence rate using shuffling.

Our work paves the way for a better understanding of the seemingly unreasonable effect of data heterogeneity in FL. The theoretical findings inspired us to present a more practical framework, which shuffles the locally generated synthetic dataset, achieving nearly as good performance as centralized learning, even when the data heterogeneity is high in some cases. Our work reveals the importance of data distribution matching in FL, opening up future research directions.

Acknowledgments and Disclosure of Funding

Bo Li, Mikkel N. Schmidt, and Tommy S. Alstrøm thank for financial support from the European Union’s Horizon 2020 research and innovation programme under grant agreement no. 883390 (H2020-SU-SECU-2019 SERSing Project). Sebastian Stich thanks for partial financial support from a Meta Privacy Enhancing Technologies Research Award 2022. Bo Li thanks for the financial support from the Otto Mønsted Foundation and appreciates the discussion with Xiaowen Jiang.

References

- [1] M. Abadi, A. Chu, I. Goodfellow, H. B. McMahan, I. Mironov, K. Talwar, and L. Zhang. Deep learning with differential privacy. In *Proceedings of the 2016 ACM SIGSAC conference on computer and communications security*, pages 308–318, 2016.
- [2] D. A. E. Acar, Y. Zhao, R. M. Navarro, M. Mattina, P. N. Whatmough, and V. Saligrama. Federated learning based on dynamic regularization. In *9th International Conference on Learning Representations, ICLR 2021, Virtual Event, Austria, May 3-7, 2021*. OpenReview.net, 2021.
- [3] C. P. Burgess, I. Higgins, A. Pal, L. Matthey, N. Watters, G. Desjardins, and A. Lerchner. Understanding disentangling in beta-vae, 2018.
- [4] Z. B. Charles, Z. Garrett, Z. Huo, S. Shmulyian, and V. Smith. On large-cohort training for federated learning. In *Neural Information Processing Systems*, 2021.
- [5] D. Chen, T. Orekondy, and M. Fritz. GS-WGAN: A gradient-sanitized approach for learning differentially private generators. In H. Larochelle, M. Ranzato, R. Hadsell, M. Balcan, and H. Lin, editors, *Advances in Neural Information Processing Systems 33: Annual Conference on Neural Information Processing Systems 2020, NeurIPS 2020, December 6-12, 2020, virtual*, 2020.
- [6] H.-Y. Chen, C.-H. Tu, Z. Li, H. W. Shen, and W.-L. Chao. On the importance and applicability of pre-training for federated learning. In *The Eleventh International Conference on Learning Representations*, 2023.
- [7] L. Collins, H. Hassani, A. Mokhtari, and S. Shakkottai. Fedavg with fine tuning: Local updates lead to representation learning. In A. H. Oh, A. Agarwal, D. Belgrave, and K. Cho, editors, *Advances in Neural Information Processing Systems*, 2022.
- [8] J. Goetz and A. Tewari. Federated learning via synthetic data. *CoRR*, abs/2008.04489, 2020.
- [9] I. Goodfellow, J. Pouget-Abadie, M. Mirza, B. Xu, D. Warde-Farley, S. Ozair, A. Courville, and Y. Bengio. Generative adversarial nets. In Z. Ghahramani, M. Welling, C. Cortes, N. Lawrence, and K. Weinberger, editors, *Advances in Neural Information Processing Systems*, volume 27. Curran Associates, Inc., 2014.
- [10] K. He, X. Zhang, S. Ren, and J. Sun. Deep residual learning for image recognition. In *2016 IEEE Conference on Computer Vision and Pattern Recognition, CVPR 2016, Las Vegas, NV, USA, June 27-30, 2016*, pages 770–778. IEEE Computer Society, 2016.
- [11] J. Ho, A. Jain, and P. Abbeel. Denoising diffusion probabilistic models. *arXiv preprint arxiv:2006.11239*, 2020.

- [12] P. Kairouz, H. B. McMahan, B. Avent, A. Bellet, M. Bennis, A. N. Bhagoji, K. A. Bonawitz, Z. Charles, G. Cormode, R. Cummings, R. G. L. D’Oliveira, S. E. Rouayheb, D. Evans, J. Gardner, Z. Garrett, A. Gascón, B. Ghazi, P. B. Gibbons, M. Gruteser, Z. Harchaoui, C. He, L. He, Z. Huo, B. Hutchinson, J. Hsu, M. Jaggi, T. Javidi, G. Joshi, M. Khodak, J. Konečný, A. Korolova, F. Koushanfar, S. Koyejo, T. Lepoint, Y. Liu, P. Mittal, M. Mohri, R. Nock, A. Özgür, R. Pagh, M. Raykova, H. Qi, D. Ramage, R. Raskar, D. Song, W. Song, S. U. Stich, Z. Sun, A. T. Suresh, F. Tramèr, P. Vepakomma, J. Wang, L. Xiong, Z. Xu, Q. Yang, F. X. Yu, H. Yu, and S. Zhao. Advances and open problems in federated learning. *CoRR*, abs/1912.04977, 2019.
- [13] S. P. Karimireddy, M. Jaggi, S. Kale, M. Mohri, S. J. Reddi, S. U. Stich, and A. T. Suresh. Mime: Mimicking centralized stochastic algorithms in federated learning. *CoRR*, abs/2008.03606, 2020.
- [14] S. P. Karimireddy, S. Kale, M. Mohri, S. Reddi, S. Stich, and A. T. Suresh. SCAFFOLD: Stochastic controlled averaging for federated learning. In H. D. III and A. Singh, editors, *Proceedings of the 37th International Conference on Machine Learning*, volume 119 of *Proceedings of Machine Learning Research*, pages 5132–5143. PMLR, 13–18 Jul 2020.
- [15] T. Karras, M. Aittala, J. Hellsten, S. Laine, J. Lehtinen, and T. Aila. Training generative adversarial networks with limited data. *CoRR*, abs/2006.06676, 2020.
- [16] A. Khaled, K. Mishchenko, and P. Richtárik. Better communication complexity for local SGD. *CoRR*, abs/1909.04746, 2019.
- [17] A. Khaled, K. Mishchenko, and P. Richtárik. Tighter theory for local sgd on identical and heterogeneous data. In *International Conference on Artificial Intelligence and Statistics*, pages 4519–4529. PMLR, 2020.
- [18] D. P. Kingma and M. Welling. Auto-encoding variational bayes. *CoRR*, abs/1312.6114, 2013.
- [19] A. Koloskova, N. Loizou, S. Boreiri, M. Jaggi, and S. Stich. A unified theory of decentralized SGD with changing topology and local updates. In H. D. III and A. Singh, editors, *Proceedings of the 37th International Conference on Machine Learning*, volume 119 of *Proceedings of Machine Learning Research*, pages 5381–5393. PMLR, 13–18 Jul 2020.
- [20] J. Konečný, H. B. McMahan, D. Ramage, and P. Richtárik. Federated optimization: Distributed machine learning for on-device intelligence. *CoRR*, abs/1610.02527, 2016.
- [21] A. Krizhevsky. Learning multiple layers of features from tiny images. 2009.
- [22] Y. LeCun and C. Cortes. MNIST handwritten digit database. 2010.
- [23] B. Li, M. N. Schmidt, T. S. Alstrøm, and S. U. Stich. Partial variance reduction improves non-convex federated learning on heterogeneous data. *CoRR*, abs/2212.02191, 2022.
- [24] Z. Li, J. Shao, Y. Mao, J. H. Wang, and J. Zhang. Federated learning with GAN-based data synthesis for non-IID clients, 2022.
- [25] T. Lin, L. Kong, S. U. Stich, and M. Jaggi. Ensemble distillation for robust model fusion in federated learning. In H. Larochelle, M. Ranzato, R. Hadsell, M. Balcan, and H. Lin, editors, *Advances in Neural Information Processing Systems 33: Annual Conference on Neural Information Processing Systems 2020, NeurIPS 2020, December 6-12, 2020, virtual*, 2020.
- [26] M. Luo, F. Chen, D. Hu, Y. Zhang, J. Liang, and J. Feng. No fear of heterogeneity: Classifier calibration for federated learning with non-iid data. In *Neural Information Processing Systems*, 2021.
- [27] L. Matthey, I. Higgins, D. Hassabis, and A. Lerchner. dsprites: Disentanglement testing sprites dataset. <https://github.com/deepmind/dsprites-dataset/>, 2017.
- [28] H. B. McMahan, E. Moore, D. Ramage, S. Hampson, and B. A. y Arcas. Communication-efficient learning of deep networks from decentralized data. In *International Conference on Artificial Intelligence and Statistics*, 2016.
- [29] H. B. McMahan, D. Ramage, K. Talwar, and L. Zhang. Learning differentially private recurrent language models. In *International Conference on Learning Representations*, 2018.
- [30] A. Mitra, R. Jaafar, G. J. Pappas, and H. Hassani. Linear convergence in federated learning: Tackling client heterogeneity and sparse gradients. In M. Ranzato, A. Beygelzimer, Y. Dauphin, P. Liang, and J. W. Vaughan, editors, *Advances in Neural Information Processing Systems*, volume 34, pages 14606–14619. Curran Associates, Inc., 2021.

- [31] S. J. Reddi, Z. Charles, M. Zaheer, Z. Garrett, K. Rush, J. Konečný, S. Kumar, and H. B. McMahan. Adaptive federated optimization. *CoRR*, abs/2003.00295, 2020.
- [32] A. K. Sahu, T. Li, M. Sanjabi, M. Zaheer, A. Talwalkar, and V. Smith. On the convergence of federated optimization in heterogeneous networks. *CoRR*, abs/1812.06127, 2018.
- [33] T. Salimans, I. Goodfellow, W. Zaremba, V. Cheung, A. Radford, X. Chen, and X. Chen. Improved techniques for training gans. In D. Lee, M. Sugiyama, U. Luxburg, I. Guyon, and R. Garnett, editors, *Advances in Neural Information Processing Systems*, volume 29. Curran Associates, Inc., 2016.
- [34] V. Sehwal, S. Mahloujifar, T. Handina, S. Dai, C. Xiang, M. Chiang, and P. Mittal. Robust learning meets generative models: Can proxy distributions improve adversarial robustness? In *International Conference on Learning Representations*, 2022.
- [35] M. J. Sheller, B. Edwards, G. A. Reina, J. Martin, S. Pati, A. Kotrotsou, M. Milchenko, W. Xu, D. Marcus, R. R. Colen, and S. Bakas. Federated learning in medicine: facilitating multi-institutional collaborations without sharing patient data. *Scientific Reports*, 10(1):12598, Jul 2020.
- [36] R. Shokri and V. Shmatikov. Privacy-preserving deep learning. In *Proceedings of the 22nd ACM SIGSAC Conference on Computer and Communications Security, CCS '15*, page 1310–1321, New York, NY, USA, 2015. Association for Computing Machinery.
- [37] A. Shrivastava, T. Pfister, O. Tuzel, J. Susskind, W. Wang, and R. Webb. Learning from simulated and unsupervised images through adversarial training. *CoRR*, abs/1612.07828, 2016.
- [38] A. Sinha, K. Ayush, J. Song, B. Uzket, H. Jin, and S. Ermon. Negative data augmentation. In *International Conference on Learning Representations*, 2021.
- [39] S. U. Stich. Unified optimal analysis of the (stochastic) gradient method. *CoRR*, abs/1907.04232, 2019.
- [40] H.-P. Wang, D. Chen, R. Kerkouche, and M. Fritz. Fed-gloss-dp: Federated, global learning using synthetic sets with record level differential privacy. *arXiv preprint arXiv:2302.01068*, 2023.
- [41] J. Wang, Z. Charles, Z. Xu, G. Joshi, H. B. McMahan, B. A. y Arcas, M. Al-Shedivat, G. Andrew, S. Avestimehr, K. Daly, D. Data, S. N. Diggavi, H. Eichner, A. Gadhikar, Z. Garrett, A. M. Girgis, F. Hanzely, A. Hard, C. He, S. Horváth, Z. Huo, A. Ingerman, M. Jaggi, T. Javidi, P. Kairouz, S. Kale, S. P. Karimireddy, J. Konečný, S. Koyejo, T. Li, L. Liu, M. Mohri, H. Qi, S. J. Reddi, P. Richtárik, K. Singhal, V. Smith, M. Soltanolkotabi, W. Song, A. T. Suresh, S. U. Stich, A. Talwalkar, H. Wang, B. E. Woodworth, S. Wu, F. X. Yu, H. Yuan, M. Zaheer, M. Zhang, T. Zhang, C. Zheng, C. Zhu, and W. Zhu. A field guide to federated optimization. *CoRR*, abs/2107.06917, 2021.
- [42] J. Wang, R. Das, G. Joshi, S. Kale, Z. Xu, and T. Zhang. On the unreasonable effectiveness of federated averaging with heterogeneous data, 2022.
- [43] J. Wang, Q. Liu, H. Liang, G. Joshi, and H. V. Poor. Tackling the objective inconsistency problem in heterogeneous federated optimization. *CoRR*, abs/2007.07481, 2020.
- [44] B. E. Woodworth, K. K. Patel, and N. Srebro. Minibatch vs local sgd for heterogeneous distributed learning. In H. Larochelle, M. Ranzato, R. Hadsell, M. Balcan, and H. Lin, editors, *Advances in Neural Information Processing Systems*, volume 33, pages 6281–6292. Curran Associates, Inc., 2020.
- [45] L. Xie, K. Lin, S. Wang, F. Wang, and J. Zhou. Differentially private generative adversarial network. *CoRR*, abs/1802.06739, 2018.
- [46] Y. Xiong, R. Wang, M. Cheng, F. Yu, and C.-J. Hsieh. FedDM: Iterative distribution matching for communication-efficient federated learning, 2023.
- [47] J. Yoon, J. Jordon, and M. van der Schaar. PATE-GAN: Generating synthetic data with differential privacy guarantees. In *International Conference on Learning Representations*, 2019.
- [48] Y. Yu, A. Wei, S. P. Karimireddy, Y. Ma, and M. Jordan. TCT: Convexifying federated learning using bootstrapped neural tangent kernels. In A. H. Oh, A. Agarwal, D. Belgrave, and K. Cho, editors, *Advances in Neural Information Processing Systems*, 2022.
- [49] J. Zhang, C. Chen, B. Li, L. Lyu, S. Wu, S. Ding, C. Shen, and C. Wu. DENSE: Data-free one-shot federated learning. In A. H. Oh, A. Agarwal, D. Belgrave, and K. Cho, editors, *Advances in Neural Information Processing Systems*, 2022.

- [50] S. Zhao, Z. Liu, J. Lin, J. Zhu, and S. Han. Differentiable augmentation for data-efficient GAN training. *CoRR*, abs/2006.10738, 2020.
- [51] Y. Zhao, M. Li, L. Lai, N. Suda, D. Civin, and V. Chandra. Federated learning with non-iid data. *arXiv preprint arXiv:1806.00582*, 2018.
- [52] Z. Zhu, J. Hong, and J. Zhou. Data-free knowledge distillation for heterogeneous federated learning. *CoRR*, abs/2105.10056, 2021.

Appendix

A Extra related work comparison

Table A.1: Comparison with the existing approaches that use synthetic data in FL. Our proposed method is easy to use and has removed many other complicated components from the existing methods.

	Local \mathcal{G}_i	Server \mathcal{G}	$\tilde{\mathcal{D}}(r)$	$\mathbf{x} \leftarrow \tilde{\mathcal{D}}$	Pseudo-label
FedDM [46]	✓	✗	✓	✓	✗
FedGEN [52]	✗	✓	✓	✗	✗
Dense [49]	✗	✓	✗	✓	✗
SDA-FL [24]	✓	✗	✓	✓	✓
ours	✓	✗	✗	✗	✗

¹ $\tilde{\mathcal{D}}(r)$: transmit the synthetic dataset every round

² $\mathbf{x} \leftarrow \tilde{\mathcal{D}}$: updates the server model \mathbf{x} with $\tilde{\mathcal{D}}$ every round

Local \mathcal{G}_i and Server \mathcal{G} means local and server generators for generating synthetic datasets. $\tilde{\mathcal{D}}(r)$ means the synthetic data is transmitted between the client and server at every communication round, which can incur extra communication costs. Updating the server model with the synthetic data at every communication round $\mathbf{x} \leftarrow \tilde{\mathcal{D}}$ requires the synthetic data to be of high quality [25, 34], as updating the server model with low-quality synthetic data or synthetic data with a different distribution than the actual local data may discard the valuable information it has learned.

B Extra experimental details

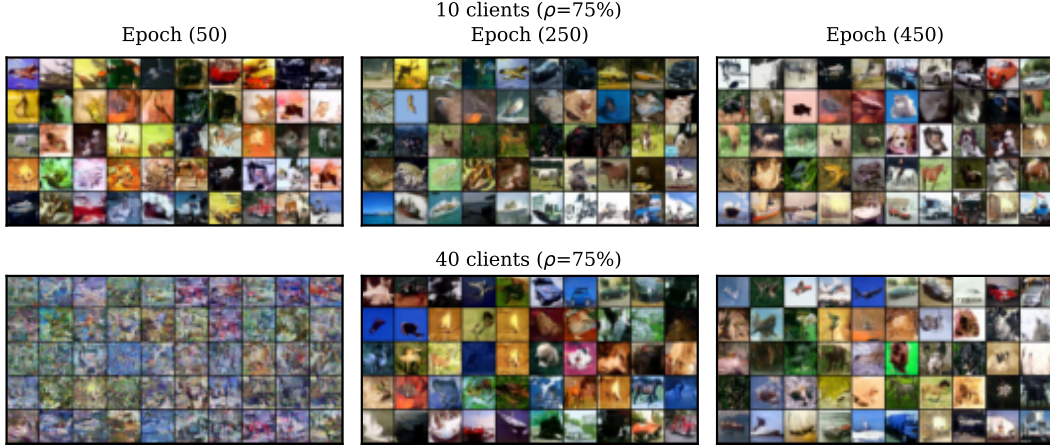


Figure B.1: Example simulated images from different training epochs on CIFAR10. The number of training images per client is 3375 for the top row and 875 for the bottom row. When the number of clients is small and the number of training images for training DDPM is high, the images extracted from Epoch 50 are already high quality. However, when the number of clients is high, the longer we train the DDPM, the better images we can obtain.

Experimental results on MNIST dataset We consider a distributed multi-class classification problem on MNIST dataset given (A_i, \mathbf{b}_i) as the dataset on worker i with:

$$\mathbf{y}_i = \text{softmax}(A_i \mathbf{x}), \quad A_i \sim \mathbb{R}^{n_i \times 784}, \mathbf{x} \in \mathbb{R}^{784 \times 10}, \mathbf{y}_i \in \mathbb{R}^{n_i \times 10} \quad (\text{B.1a})$$

$$f_i(\mathbf{x}) := \frac{1}{n_i} \sum_{j=1}^{n_i} \frac{1}{10} \sum_{k=1}^{10} (\mathbf{b}_{ijk} \log(\mathbf{y}_{ijk})) \quad (\text{B.1b})$$

We construct the training dataset by subsampling 1024 images from each class from the MNIST training dataset. We use the test dataset to evaluate the performance of the server model (10000 images). We consider two scenarios for splitting the dataset across workers: 1) `iid`, where each worker has a similar number of images across classes 2) `split by class`, where each worker can only see images from a single class. We set 10 workers, and each worker has 1024 images $n_i = 1024$. We experiment with a different number of local epochs E on each worker and shuffling percentage p . For a given p , we subsample $n_i p$ data points randomly from each worker and allocate them in \tilde{D} . We then shuffle \tilde{D} and distribute it equally to all workers such that each worker has $n_i p$ shuffled data points and $n_i(1 - p)$ local data points. We choose to control the stochastic noise $\bar{\sigma}^2$ by adding Gaussian noise to every gradient:

$$\mathbf{y}_i \leftarrow \mathbf{y}_i - \eta(\nabla f_i(\mathbf{y}_i) + s), \quad s \sim \mathcal{N}(0, \frac{\bar{\sigma}^2}{784}) \tag{B.2}$$

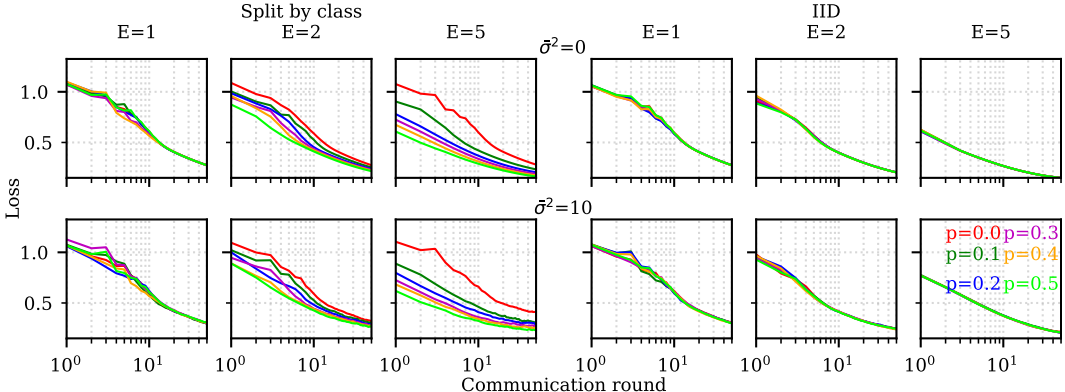


Figure B.2: Test loss using the server model over communication rounds. When the dataset is IID across workers, adding shuffled dataset does not influence the learning speed. However, when workers have heterogeneous datasets (`split by class`), shuffling a small percentage of the dataset can improve the convergence speed, especially when the number of local epochs is high (*e.g.* $E = 5$)

Fig. B.2 shows the results. When the dataset is IID across workers, adding the shuffled dataset to each worker does not influence the learning speed. This agrees with the lemmas that we have shown in the main text. When the dataset is non-iid across workers, shuffling a small percentage of the local dataset can highly improve the convergence, especially when the number of local epochs is high, *e.g.* $E = 5$. We can achieve a slightly better speedup when the stochastic noise is non-zero, which is most of the cases in the neural network training where we use mini-batch SGD.

Extra figure for Sec. 2.3 Fitted lines between the number of iterations and $\frac{1}{\sqrt{\epsilon}}$.

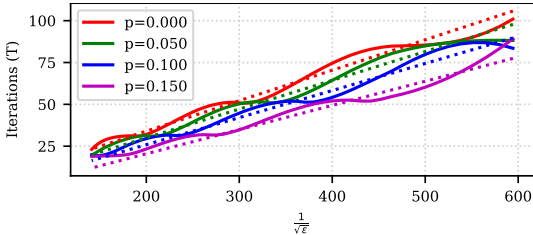


Figure B.3: Fitted lines between the number of iterations and $\frac{1}{\sqrt{\epsilon}}$

Limitations As our proposed framework requires the uploading of the synthetic data to the server, it is less appropriate for tasks that deal with substantially sensitive information, such as patient records. A possible way to improve the utility of our proposed framework is to make the generator and federated learning algorithms differential private. We leave this as our future work.

C Experimental results on dSprites dataset

In this section, we demonstrate the effectiveness of our proposed framework on the dSprites dataset [27]. We here perform a slightly different synthetic data generation process. Rather than using the DDPM [11], we generate the synthetic dataset on each client with β -VAE [3]. We then aggregate and shuffle the collected synthetic dataset on the server and distribute them to clients following the same procedure as described in Sec. 3 and Sec. 4.

C.1 Training details

The dSprites dataset [27] contains three different types of shapes with different colours, scales, rotations, and locations.

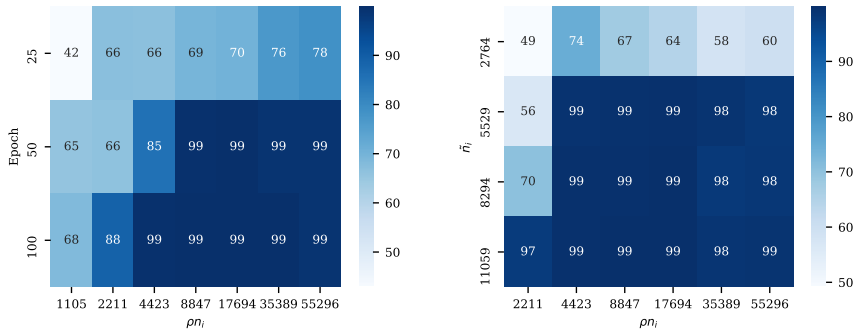


Figure C.1: Performance on the dSprites test dataset. Left: the influence of the number of training epochs and training images (ρn_i) in training the generator on the FL performance. Right: the influence of the number of synthetic images (\tilde{n}_i) on the FL performance. When we use fewer training images to train the generator (e.g. 2211), it is beneficial to train the generator longer and sample more synthetic images.

Data preparation We first randomly select 10% of the images from the dSprites dataset to formulate the test set. We leave the test set on the server to evaluate the performance of the server model. For the rest of the dataset, we split them among 12 clients ($N = 12$) based on the four spatial locations (top-left, bottom-left, top-right, or bottom-right) and three shapes (square, ellipse, or heart) such that each client only sees a single type of shape from one of the four pre-defined locations. The number of images on each client is the same ($n_i = 55296$). We consider each shape as a class and perform shape classification.

Synthetic data generation We use β -VAE with the same architecture as [3] following a publicly available implementation⁵. We train an individual β -VAE [3] on each client with batch size 256, latent dimension 10. To evaluate the sensitivity of the federated learning optimization on the quality of the generator, we train the generator using different fractions of data ρn_i with ρ being $\{1\%, 2\%, 4\%, 8\%, 16\%, 32\%, 64\%, 100\%\}$ on each client. When $\rho = 100\%$, we train a β -VAE with the entire dataset from each client.

Many works have demonstrated that the latent variables in β -VAE can encode disentangled representative features of the input images [3, 27, 18], and manipulating a single latent dimension can result in substantial changes of the corresponding factor of variation, e.g. scale, in the output from the decoder. Therefore, we can obtain diverse synthetic images by interpolating the extracted latent representations. To achieve this, we extract the averaged latent representations for each class, specifically the mean of the posterior distribution μ_c [3]. We then sample \tilde{n}_i latent codes from the Gaussian distribution parameterised by mean μ_c and standard deviation 1. The sampled latent codes are then passed as the input for the decoder from β -VAE to generate synthetic images. We collect the synthetic images from all the clients, which are then shuffled and distributed equally to each client such that the local dataset on each client is $p\mathcal{D}_i + (1-p)\tilde{\mathcal{D}}_{si}$. An example of the generated synthetic image is shown in Fig. C.2. With the updated dataset on each client, we follow the same procedure as documented in Sec. 4 to perform federated optimization with FedAvg [28]. We make this dataset publicly available at <https://github.com/mlolab/fedssyn-synthetic-dSprites>.

⁵<https://github.com/1Konny/Beta-VAE/>

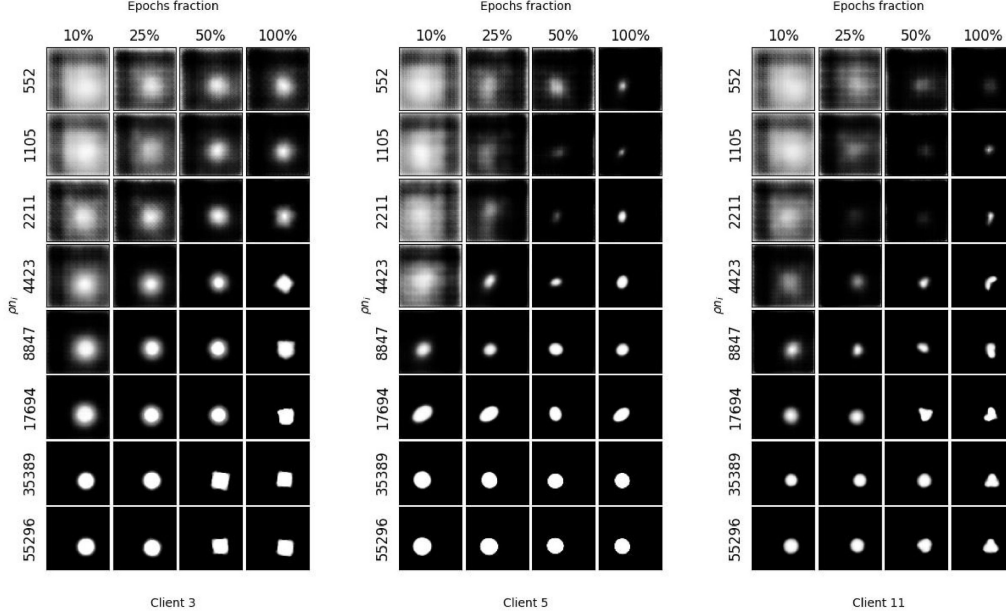


Figure C.2: Example synthetic images from clients 3, 5, and 11. The x-axis shows the training fraction of 360 epochs, and the y-axis shows the number of training images used to train the generator. The number of training images has a more substantial influence on the quality of the synthetic data.

C.2 Discussion

We show the sensitivity of FedAvg’s performance on the quality of the synthetic images in Fig. C.1. The left image shows that training the VAE longer does not necessarily provide better quality synthetic images when we use fewer training images. However, when we use more training images (higher ρ), the images extracted from early checkpoints, *e.g.* 50% epochs, are already of high quality. We observe a similar pattern in the right image in Fig. C.1, where the number of training images has a more substantial influence on the performance of FedAvg than the number of generated synthetic images.

D Proof

We provide the proof and some extra definitions for carrying out the proof in this section.

Table D.1: Summary of notations used in the proof

\mathcal{D}_i	local data distribution on client i
$\tilde{\mathcal{D}}$	shuffled data distribution on client i
$\hat{\mathcal{D}}_i := (1 - p)\mathcal{D}_i + p\tilde{\mathcal{D}}$	effective data distribution client i
f, \hat{f}_i, F_i	functions evaluated on the data distribution \mathcal{D}_i
$\tilde{f}, \tilde{\hat{f}}_i, \tilde{F}_i$	functions evaluated on the data distribution $\tilde{\mathcal{D}}$
$\hat{f}, \hat{\hat{f}}_i, \hat{F}_i$	functions evaluated on the data distribution $\hat{\mathcal{D}}_i$

Table D.1 shows the summary of the notations. We assume each client has access to data with distribution \mathcal{D}_i that is non-iid across clients and we denote by $\tilde{\mathcal{D}} := \cup_i \mathcal{D}_i$ the uniform distribution over the join data. We define a random variable $b \in \{0, 1\}$ that indicates where a data point is drawn from. When $b = 0$ (with probability $1 - p$), we assume that we draw data from the worker’s own distribution \mathcal{D}_i . When $b = 1$ (with probability p), we assume data is drawn from the the uniform

distribution $\tilde{\mathcal{D}}$.

$$\hat{F}_i(\mathbf{x}; b, \mathcal{D}_i, \tilde{\mathcal{D}}) := \begin{cases} F_{i, \xi \sim \mathcal{D}_i}(\mathbf{x}; \xi | b = 0) & \text{with probability } 1 - p \\ \tilde{F}_{i, \xi \sim \tilde{\mathcal{D}}}(\mathbf{x}; \xi | b = 1) & \text{with probability } p \end{cases} \quad (\text{D.1})$$

For simplicity, we will omit ξ . Take the expectation with respect to b in Eq. D.1, we obtain:

$$\hat{F}_i(\mathbf{x}; \mathcal{D}_i, \tilde{\mathcal{D}}) = \mathbb{E}_b[\hat{F}_i(\mathbf{x}; b, \mathcal{D}_i, \tilde{\mathcal{D}})] = (1 - p)F_i(\mathbf{x}; \mathcal{D}_i) + p\tilde{F}_i(\mathbf{x}; \tilde{\mathcal{D}}) \quad (\text{D.2a})$$

$$\begin{aligned} \hat{f}_i(\mathbf{x}) &:= \mathbb{E}_{\mathcal{D}_i, \tilde{\mathcal{D}}}[\hat{F}_i(\mathbf{x}; \mathcal{D}_i, \tilde{\mathcal{D}})] = (1 - p)\mathbb{E}_{\mathcal{D}_i}[F_i(\mathbf{x})] + p\mathbb{E}_{\tilde{\mathcal{D}}}[\tilde{F}_i(\mathbf{x})] \\ &= (1 - p)f_i(\mathbf{x}) + p\tilde{f}_i(\mathbf{x}) \end{aligned} \quad (\text{D.2b})$$

$$\hat{f}(\mathbf{x}) := \mathbb{E}[\hat{f}_i(\mathbf{x})] = \mathbb{E}[(1 - p)f_i(\mathbf{x}) + p\tilde{f}_i(\mathbf{x})] = (1 - p)f(\mathbf{x}) + p\tilde{f}(\mathbf{x}) \quad (\text{D.2c})$$

Lemma D-1 (variance with probability). *If the random variable X is discrete with each element x_i appearing with a probability p_i such that $p(x_i) = p_i$, then:*

$$\mathbb{E}\|X - \mu\|^2 = \sum_{i=1}^n p_i \|x_i - \mu\|^2, \quad \mu := \frac{1}{n} \sum_{i=1}^n p_i x_i. \quad (\text{D.3})$$

Lemma D-2 (shuffled gradient dissimilarity). *If Assumption 1 holds, then $\forall \mathbf{x} \in \mathbb{R}^d$:*

$$\hat{\zeta}_p^2 := \mathbb{E}\|\nabla \hat{f}_i(\mathbf{x}) - \nabla \hat{f}(\mathbf{x})\|^2 \leq (1 - p)^2 \zeta^2. \quad (\text{D.4})$$

Proof. Given the definition from Eq. D.2, we have:

$$\begin{aligned} \hat{\zeta}_p^2 &:= \mathbb{E}\|\nabla \hat{f}_i(\mathbf{x}) - \nabla \hat{f}(\mathbf{x})\|^2 \\ &= \mathbb{E}\|(1 - p)\nabla f_i(\mathbf{x}) + p\nabla \tilde{f}_i(\mathbf{x}) - (1 - p)\nabla f(\mathbf{x}) - p\nabla \tilde{f}(\mathbf{x})\|^2 \\ &= (1 - p)^2 \mathbb{E}\|\nabla f_i(\mathbf{x}) - \nabla f(\mathbf{x})\|^2 + p^2 \mathbb{E}\|\nabla \tilde{f}_i(\mathbf{x}) - \nabla \tilde{f}(\mathbf{x})\|^2 \\ &\leq (1 - p)^2 \zeta^2. \end{aligned} \quad (\text{D.5})$$

By definition, the gradient dissimilarity is 0, $\mathbb{E}\|\nabla \tilde{f}_i(\mathbf{x}) - \nabla \tilde{f}(\mathbf{x})\|^2 = 0$ when the data is iid across clients. \square

Lemma D-3 (shuffled stochastic noise). *If Assumption 1 and 2 hold and let $\tilde{\sigma}^2$ being the stochastic noise from using $\tilde{\mathcal{D}}$, let $\delta^2 := \|\nabla f(\mathbf{x}) - \nabla \tilde{f}(\mathbf{x})\|^2$, then $\forall \mathbf{x} \in \mathbb{R}^d$, we have:*

$$\mathbb{E}\hat{\sigma}_p^2 \leq (1 - p)\sigma^2 + p\tilde{\sigma}^2 + p(1 - p)\zeta^2 + p(1 - p)\delta^2. \quad (\text{D.6})$$

Proof. Based on the definition in Eq. D.2, we have:

$$\begin{aligned} \hat{\sigma}_p^2 &:= \mathbb{E}_{\mathcal{D}_i, \tilde{\mathcal{D}}}\|\nabla \hat{F}_i(\mathbf{x}) - \nabla \hat{f}_i(\mathbf{x})\|^2 \\ &= \mathbb{E}_{\mathcal{D}_i, \tilde{\mathcal{D}}}\|(1 - p)\nabla F_i(\mathbf{x}) + p\nabla \tilde{F}_i(\mathbf{x}) - \nabla \hat{f}_i(\mathbf{x})\|^2 \\ &= (1 - p) \underbrace{\mathbb{E}_{\mathcal{D}_i, \tilde{\mathcal{D}}}\|\nabla F_i(\mathbf{x}) - \nabla \hat{f}_i(\mathbf{x})\|^2}_{\mathcal{A}_1} + p \underbrace{\mathbb{E}_{\mathcal{D}_i, \tilde{\mathcal{D}}}\|\nabla \tilde{F}_i(\mathbf{x}) - \nabla \hat{f}_i(\mathbf{x})\|^2}_{\mathcal{A}_2}. \end{aligned} \quad (\text{D.7})$$

In the last inequality, we use Lemma D-1.

$$\begin{aligned} \mathcal{A}_1 &= \mathbb{E}_{\mathcal{D}_i, \tilde{\mathcal{D}}}\|\nabla F_i(\mathbf{x}) - \nabla f_i(\mathbf{x}) + \nabla f_i(\mathbf{x}) - \nabla \hat{f}_i(\mathbf{x})\|^2 \\ &= \mathbb{E}_{\mathcal{D}_i}\|\nabla F_i(\mathbf{x}) - \nabla f_i(\mathbf{x})\|^2 + \|\nabla f_i(\mathbf{x}) - \nabla \hat{f}_i(\mathbf{x})\|^2 \\ &\leq \sigma^2 + \|\nabla f_i(\mathbf{x}) - (1 - p)\nabla f_i(\mathbf{x}) - p\nabla \tilde{f}_i(\mathbf{x})\|^2 \\ &= \sigma^2 + p^2\|\nabla f_i(\mathbf{x}) - \nabla \tilde{f}_i(\mathbf{x})\|^2. \end{aligned} \quad (\text{D.8})$$

The second equality uses the condition that $\mathbb{E}_{\mathcal{D}_i}[\nabla F_i(\mathbf{x})] - \nabla f_i(\mathbf{x}) = 0$, similarly, we can bound \mathcal{A}_2 as following:

$$\begin{aligned}
\mathcal{A}_2 &= \mathbb{E}_{\mathcal{D}_i, \tilde{\mathcal{D}}} \|\nabla \tilde{F}_i(\mathbf{x}) - \nabla \tilde{f}_i(\mathbf{x}) + \nabla \tilde{f}_i(\mathbf{x}) - \nabla \hat{f}_i(\mathbf{x})\|^2 \\
&= \mathbb{E}_{\tilde{\mathcal{D}}} \|\nabla \tilde{F}_i(\mathbf{x}) - \nabla \tilde{f}_i(\mathbf{x})\|^2 + \|\nabla \tilde{f}_i(\mathbf{x}) - \nabla \hat{f}_i(\mathbf{x})\|^2 \\
&\leq \tilde{\sigma}^2 + \|\nabla \tilde{f}_i(\mathbf{x}) - (1-p)\nabla f_i(\mathbf{x}) - p\nabla \tilde{f}_i(\mathbf{x})\|^2 \\
&= \tilde{\sigma}^2 + (1-p)^2 \|\nabla f_i(\mathbf{x}) - \nabla \tilde{f}_i(\mathbf{x})\|^2.
\end{aligned} \tag{D.9}$$

Take the bound of \mathcal{A}_1 and \mathcal{A}_2 back to Eq. D.7, we get:

$$\begin{aligned}
\hat{\sigma}_p^2 &\leq (1-p)\sigma^2 + (1-p)p^2 \|\nabla f_i(\mathbf{x}) - \nabla \tilde{f}_i(\mathbf{x})\|^2 + p\tilde{\sigma}^2 + p(1-p)^2 \|\nabla f_i(\mathbf{x}) - \nabla \tilde{f}_i(\mathbf{x})\|^2 \\
&\leq (1-p)\sigma^2 + p\tilde{\sigma}^2 + p(1-p) \|\nabla f_i(\mathbf{x}) - \nabla \tilde{f}_i(\mathbf{x})\|^2.
\end{aligned} \tag{D.10}$$

$$\begin{aligned}
\mathbb{E}[\hat{\sigma}_p^2] &\leq (1-p)\mathbb{E}[\sigma^2] + p\mathbb{E}[\tilde{\sigma}^2] + p(1-p)\mathbb{E}\|\nabla f_i(\mathbf{x}) - \nabla \tilde{f}_i(\mathbf{x})\|^2 \\
&= (1-p)\sigma^2 + p\tilde{\sigma}^2 + p(1-p)\mathbb{E}\|\nabla f_i(\mathbf{x}) - \nabla \tilde{f}_i(\mathbf{x})\|^2 \\
&= (1-p)\sigma^2 + p\tilde{\sigma}^2 + p(1-p)\mathbb{E}\|\nabla f_i(\mathbf{x}) - \nabla f(\mathbf{x})\|^2 + p(1-p)\mathbb{E}\|\nabla f(\mathbf{x}) - \nabla \tilde{f}_i(\mathbf{x})\|^2 \\
&\leq (1-p)\sigma^2 + p\tilde{\sigma}^2 + p(1-p)\zeta^2 + p(1-p)\delta^2.
\end{aligned} \tag{D.11}$$

The second equality uses the condition that $\mathbb{E}[\nabla f_i(\mathbf{x})] - \nabla f(\mathbf{x}) = 0$. The last inequality uses Assumption 1 and the definition of the quality $\delta^2 := \|\nabla f(\mathbf{x}) - \nabla \tilde{f}_i(\mathbf{x})\|^2$. If we create the uniform data distribution $\tilde{\mathcal{D}}$ by e.g. collecting data from other source, then we can use δ to represent the distribution difference between \mathcal{D} and $\tilde{\mathcal{D}}$. □

Lemma D-4 (shuffled smoothness). *Let L_{\max} and L_{avg} denote the maximum and average smoothness across all individual loss functions, i.e. it holds*

$$\|\nabla f_i(\mathbf{x}) - \nabla f_i(\mathbf{y})\| \leq L_{\max} \|\mathbf{x} - \mathbf{y}\|, \quad \forall \mathbf{x}, \mathbf{y} \in \mathbb{R}^d, i \in [n],$$

and

$$\|\nabla f(\mathbf{x}) - \nabla f(\mathbf{y})\| \leq L_{\text{avg}} \|\mathbf{x} - \mathbf{y}\|, \quad \forall \mathbf{x}, \mathbf{y} \in \mathbb{R}^d.$$

Then we have:

$$\mathbb{E}L_p \leq (1-p)L_{\max} + pL_{\text{avg}},$$

where $\mathbb{E}L_p$ denotes an upper bound on the smoothness constant of $\hat{f}_i(\mathbf{x})$.

Proof. For a given client index i , we verify, by definition of $\hat{f}_i(\mathbf{x}) = (1-p)f_i(\mathbf{x}) + pf(\mathbf{x})$,

$$\begin{aligned}
\left\| \nabla \hat{f}_i(\mathbf{x}) - \nabla \hat{f}_i(\mathbf{y}) \right\| &= \left\| (1-p)(\nabla f_i(\mathbf{x}) - \nabla f_i(\mathbf{y})) + p(\nabla f(\mathbf{x}) - \nabla f(\mathbf{y})) \right\| \\
&\leq (1-p) \|\nabla f_i(\mathbf{x}) - \nabla f_i(\mathbf{y})\| + p \|\nabla f(\mathbf{x}) - \nabla f(\mathbf{y})\| \\
&\leq ((1-p)L_{\max} + pL_{\text{avg}}) \cdot \|\mathbf{x} - \mathbf{y}\|.
\end{aligned} \tag{□}$$